

# Bimodal distribution of filler on viscosity and thermal expansion of glass composites

Sneha Samal, Sunghwan Cho, Hyungsun Kim\*

*School of Material Science and Engineering, Inha University, Incheon 402-751, Republic of Korea*

Received 2 July 2012; received in revised form 3 August 2012; accepted 3 August 2012

Available online 11 August 2012

## Abstract

This paper investigates the bimodal oxide filler system to study the viscous behavior and thermal expansion properties of glass composites. Zinc oxide and cordierite, which are two types of filler, with different average diameters (10  $\mu\text{m}$  and 1  $\mu\text{m}$ , respectively), were considered in a  $\text{Bi}_2\text{O}_3$  containing glass with various volume fractions (up to 40 vol%). The experimental results for the composites with the bimodal filler distribution show a reduced viscosity. The viscosity increased from fine particles to coarse particles with an increase in the volume fraction of the composite. Both viscosity and coefficient of thermal expansion (CTE) decreased significantly in the composite with the cordierite filler. The CTE is determined from the volume fraction with respect to particle size and distribution. On the other hand, viscosity is dependent on the particle distribution, particle size, and volume fraction of the composite.

© 2012 Elsevier Ltd and Techna Group S.r.l. All rights reserved.

**Keywords:** B. Composite; D. Glass; Oxide filler; Viscosity

## 1. Introduction

Currently, glass-filler composites are used for applications such as semiconductor packaging, low temperature co-fired ceramics, and display panels [1]. The preparation of suitable glass-filler composites is controlled by glass flow and viscosity. The study of glass viscosity from the transformation stage to the working temperature stage involves crucial steps that relate to the behavior of the seal [2]. Fig. 1 displays a schematic presentation of the sealing behavior of a glass-filler composite. The first phase consists of the firing stage of the glass-filler composite, and the second stage represents sealing with the filler distribution in the matrix.

Some researchers have implicated various properties, such as dielectric, thermal, and coefficient of thermal expansion (CTE) of the composite, by using bimodal distribution in polymer composites [3,4]. Previous researchers [5] studied the co-addition of oxide filler and various other types of filler to the glass composite. However, the filler of the same type with bimodal distribution in glass

composites has rarely been investigated. This paper is an extension of previous work on an earlier approach that uses filler with two mean size distributions [6].

The present investigation focuses on the bimodal filler size distribution in glass composites and the effects of filler size and distribution of the viscous and CTE behavior of these glass composites. The composites were formed by adding one or more fillers to a glass matrix in various volume fractions to control the viscous and thermal expansion properties. The filler arrangement in the liquid phase of the composite, as a function of the firing temperature with respect to viscosity, was observed. Thus, the relationship between particle size, distribution, volume fraction, viscosity, and CTE allows for key physical parameters of the composite to meet product specifications.

## 2. Experimental procedure

A glass composition was prepared with 44  $\text{Bi}_2\text{O}_3$ , 34  $\text{ZnO}$ , and 22  $\text{B}_2\text{O}_3$ . To achieve such a glass batch, the appropriate amounts of  $\text{Bi}_2\text{O}_3$  (99.9%, Aldrich),  $\text{ZnO}$  (99.9% Aldrich) and  $\text{B}_2\text{O}_3$  (99.98% Aldrich), were mixed and melted in air in an electric furnace at 1500  $^\circ\text{C}$  using an

\*Corresponding author. Tel.: +82 32 860 7545; fax: +82 32 864 3730.

E-mail address: [kimhs@inha.ac.kr](mailto:kimhs@inha.ac.kr) (H. Kim).

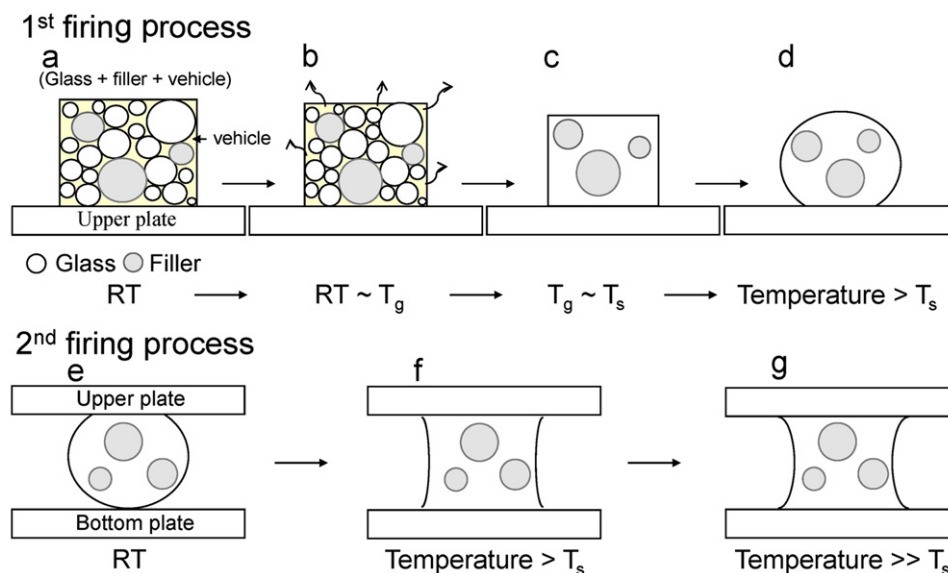


Fig. 1. Schematic diagram of the glass-filler composite that is used for sealing and the distribution of fillers in the glass matrix with respect to temperature. Sealing is used for a plasma display panel, which has a space between the two glass substrates bonded by glass powder. The sealed paste is fired at a softening temperature (a)–(d), cooled down to room temperature and then heated again for glass viscous flow (e)–(f): (a) green composite (b) after binder burn out (c) sintering of glass (d) viscous flow (e) upside down of plate (f) wetting of molten glass and (g) ideal shape of sealed.

alumina crucible. The quenched glass cullet was ball-milled to an average particle size of 100  $\mu\text{m}$  frit. Then, the frit was pulverized with a jet mill to an average particle size of 5  $\mu\text{m}$ . Commercially available cordierite and zinc oxide (Sigma-Aldrich Inc.) fillers were also considered. For both of the filler, the particle size was distributed over a wide range from coarse (10  $\mu\text{m}$ ) to fine (1  $\mu\text{m}$ ).

The glass-filler composites were prepared by adding the two fillers described above (zinc oxide and cordierite) with two broad ranges of particle sizes. The mixtures were prepared in various proportions, with 10, 20, 30, and 40 vol% fraction. The coarse and fine filler sizes were added to the glass powder with coarse to fine proportions of unity (50:50), in a bimodal filler mixtures. Zirconia balls with 3-mm diameters were added to the mixture and mixed well in a container inside a tubular mixer (Model T2 F, Glenmills, Basel, Switzerland). The arrangement of the fillers in the liquid phase of the composite were studied at various temperature ranges, from 480  $^{\circ}\text{C}$  to 580  $^{\circ}\text{C}$ , inside a sintering furnace, during a firing cycle with a 30-min holding time.

The glass transition temperature and exothermic and endothermic peaks of the glass-filler mixtures were analyzed using a differential thermal analyzer (DSC, NETZSCH, STA 449 F3). The measurements were performed in air at a heating rate of 10  $^{\circ}\text{C}/\text{min}$ . The samples were prepared by cold pressing the composite mixture. The surface morphology of the composites, after firing inside the furnace (Ajeon, S-18, sintering furnace) at 480  $^{\circ}\text{C}$  for a 10-min holding time, was analyzed with a scanning electron microscope (SEM; Hitachi S-4300). The densities of the green composites were calculated by using a pycnometer (Micromeritics, Accupyc II 1340). The crystallization phases of the green and fired composites were analyzed using XRD techniques (X-ray

diffractometer, DMAX 2500) at 4 kV with a scan speed of 2 $^{\circ}/\text{min}$ .

### 3. Results

The results of the particle size analysis (PSA) for the glass are shown with average particle size of 5  $\mu\text{m}$  (Fig. 2a). Fig. 2(c) shows the fine particle size of cordierite in the submicron range as being similar to the fine particle size of zinc oxide in Fig. 2(b). In terms of bimodal distribution, filler with coarse and fine particle sizes were chosen with broad distributions in the composite [7]. The fraction that tended toward unity showed the best results among the distributions that were tested [8,9].

In the case of bimodal filler distribution, it has been observed that fine fillers arrange themselves within the interstitial gaps of the coarse filler (Fig. 3a–d). The composite with a 40 vol% fraction of the cordierite filler exhibits an excess amount of filler within the glass matrix, which created voids in the composite (Fig. 3c). The interphases are observed in the zinc oxide-glass composite (Fig. 3d). This implicates that interphase layer results due to interaction between zinc oxide filler dissolution in the glass matrix. The zinc oxide-glass composite represent the reactive system with lighter region represents the glass matrix, darker region represents filler and the medium region represents the interphase layer. The characterizations of the composites were carried out by the XRD (Fig. 4). The composite with cordierite-glass shows amorphous nature in both green and fired conditions. On the other hand the sharp and distinct peaks are observed in zinc oxide-glass composite in both green and fired composites. Partial dissolution of the zinc oxide filler within the glass matrix was confirmed from the XRD analysis

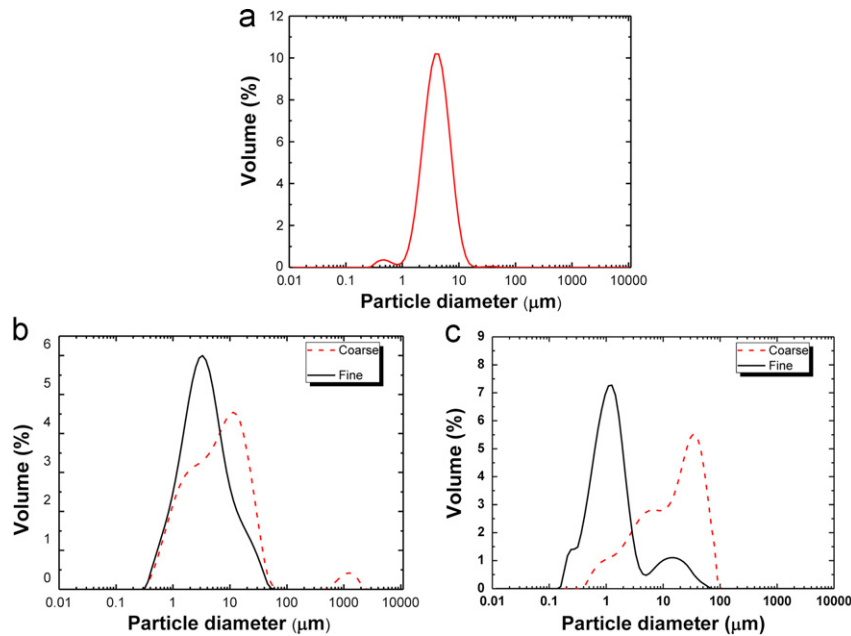


Fig. 2. PSA data of the (a) glass powder (b) zinc oxide, and (c) cordierite fillers (coarse and fine size).

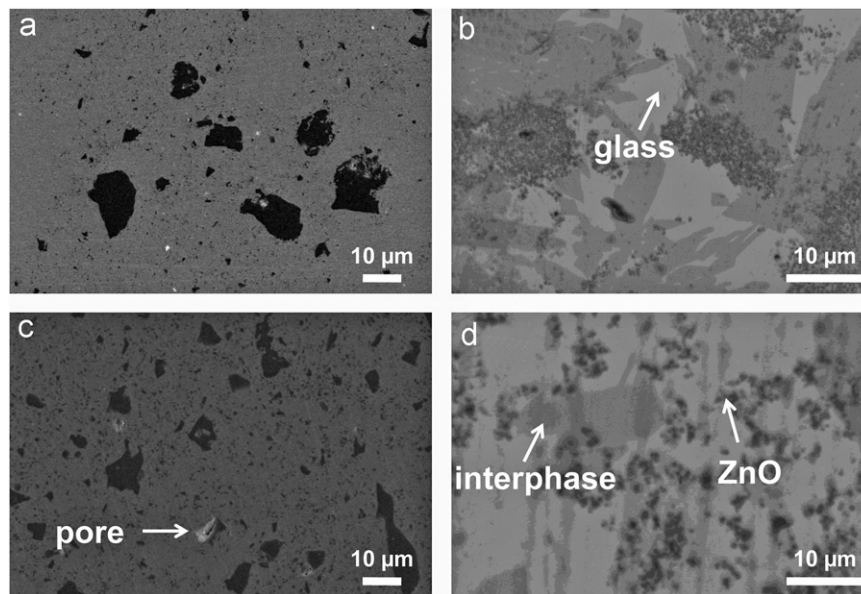


Fig. 3. SEM-SEI images of the composites sintered at 480 °C for 10 min. (a) 10 vol% cordierite-glass composite (bimodal) (b) 10 vol% zinc oxide-glass composite (bimodal) (c) 30 vol% cordierite-glass composite (bimodal) and (d) 30 vol% zinc oxide-glass composite (bimodal). (Light: glass matrix, dark: zinc oxide filler particles and medium: interphase created due to the interaction between the glass matrix and filler).

(the distinct peaks, zinc oxide ICDD PDF Card No. 96-230-0113).

The density of the glass particles ( $6.9 \text{ g/cm}^3$ ) is higher than that of filler, such as zinc oxide ( $5.7 \text{ g/cm}^3$ ) and cordierite ( $2.6 \text{ g/cm}^3$ ). As a result, the glass flows downwards due to the gravitational force of attraction. Consequently, the drift force is applied to the lighter and denser particles of the filler. The distribution of the filler in the composite occurred on the major upper portion rather than on the lower portion of the composite. Depending upon the reactivity between the glass and the filler, the

densification can be classified as a non-reactive system, partially reactive system, or completely reactive system [10,11]. Fig. 5 clearly shows that an increase in the volume fraction caused an increase in the densification after firing, whereas an increase in temperature with a higher volume fraction resulted in a decrease in the fired density due to the development of crystalline pores and cracks. Pores were observed in the zinc oxide-glass composite with 40 vol% fraction, as shown in Fig. 5. The density of the reactive system (zinc oxide-glass composite) decreased significantly when compared with the non-reactive (cordierite-glass

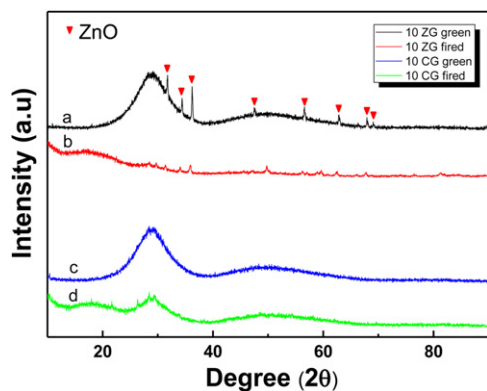


Fig. 4. Green and sintered composites at 480 °C for 30 min (a) Composite with zinc oxide as filler 10 vol% (zinc oxide ICDD PDF: 96-230-0113, not fired), (b) zinc oxide-glass composite (fired) (c) Composites with cordierite as filler 10 vol% (not fired), (d) cordierite-glass composite (fired).

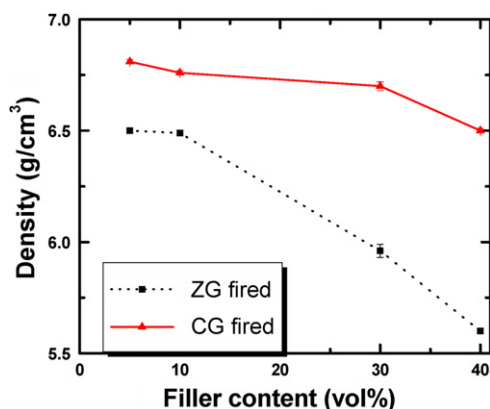


Fig. 5. Density as a function of filler content for composites (fired at 480 °C for 10 min). Density of glass particles (6.9 g/cm<sup>3</sup>), zinc oxide (5.7 g/cm<sup>3</sup>) and cordierite (2.6 g/cm<sup>3</sup>).

composite) system, which evidenced the dissolution of the filler into the glass matrix.

To observe the particle (cordierite filler) arrangement in the liquid phase of the glass matrix during the firing cycle, the composites were fired at different temperatures. The composites fired at 480 °C showed, adequate distribution of the filler throughout the glass composite without any movement. As the firing temperature was increased to 520 °C, the movement of the filler was observed (Fig. 6a<sub>1</sub>–a<sub>6</sub>). This is confirmed from the distribution of fillers on the various surfaces of the composite in the top, middle and bottom layers. Coarse fillers are observed in the top portion of the cordierite-glass composite, whereas the fine fillers are observed in the lower portion of the composite. On increasing the firing temperature to 580 °C, movement of the filler particles reverse in the liquid phase of the matrix. The fine filler observed in the top portion of the composite and coarse filler are observed in the bottom portion of the composite (Fig. 6b<sub>1</sub>–b<sub>6</sub>). The distributions of fillers from fine particles towards coarse particles are observed at various sintering temperature. This

distribution of fillers within the glass matrix correlates the viscosity of the composite.

Composites with cordierite filler showed a reduced viscosity behavior at lower temperatures (Fig. 7). The fluidity in the zinc oxide filler increased at higher temperatures due to the dissolution of filler in the glass matrix. The viscosity of the bimodal distribution of fillers was effectively reduced with respect to the monodisperse filler. At a higher volume fraction of cordierite filler, the viscosity increased very sharply due to the highly packed nature of the composite. As particle-particle interaction increased, the resistance to fluidity and creation of voids was hindered.

A higher filler content in the composite was observed to cause a significant decrease in the CTE (Fig. 8). The CTE of the composite ( $\alpha_c$ ), was calculated by using Turner's equation as follows [12]:

$$\alpha_c = \frac{\alpha_f K_f V_f + \alpha_m K_m V_m}{K_f V_f + K_m V_m} \quad (1)$$

The subscripts  $c$ ,  $m$ , and  $f$  denote the composite, matrix, and filler, respectively.  $\alpha$ ,  $K$ , and  $V$  are the CTE, bulk modulus, and volume fraction of the composite. The composite with a higher vol% fraction of filler displays a significant decrease in the CTE. The CTE of a bimodal filler-glass composite exist between the coarse and fine data of the filler-glass composite.

Fig. 9 shows the viscosity of the composite with various fillers, such as zinc oxide (reactive) and cordierite (non-reactive), that have bimodal and unimodal distribution. Viscosity decreases significantly in the bimodal filler distribution when compared with the unimodal distribution in the reactive system. On the other hand, there are some minor changes in the viscosity of the non-reactive system for the unimodal and bimodal filler distributions in the glass composite.

#### 4. Discussion

Filler-glass composites are formed by viscous flow during the liquid stage of sintering. The viscous flow of the composite is controlled by the variety and distribution of filler particle sizes. The effects of filler particle size and distribution in different orientations in the liquid phase of the glass composite have been investigated. Coarse and fine filler sizes are considered in the determination of the glass composite viscosity and CTE. Filler-glass composites with improved low-temperature sintering, thermal, and viscous properties meet the specific performance requirements of a broad range of microelectronic packaging applications. Particle size distribution influences particle packing; for example, a bimodal with a broad size distribution packs more closely than for a unimodal sample [13].

Poslinski et al. [14] showed that the shear viscosity, primary normal stress coefficient, dynamic viscosity, and storage modulus of the composites were reduced with a bimodal distribution rather than to a unimodal distribution. The concept was observed to be in agreement with the



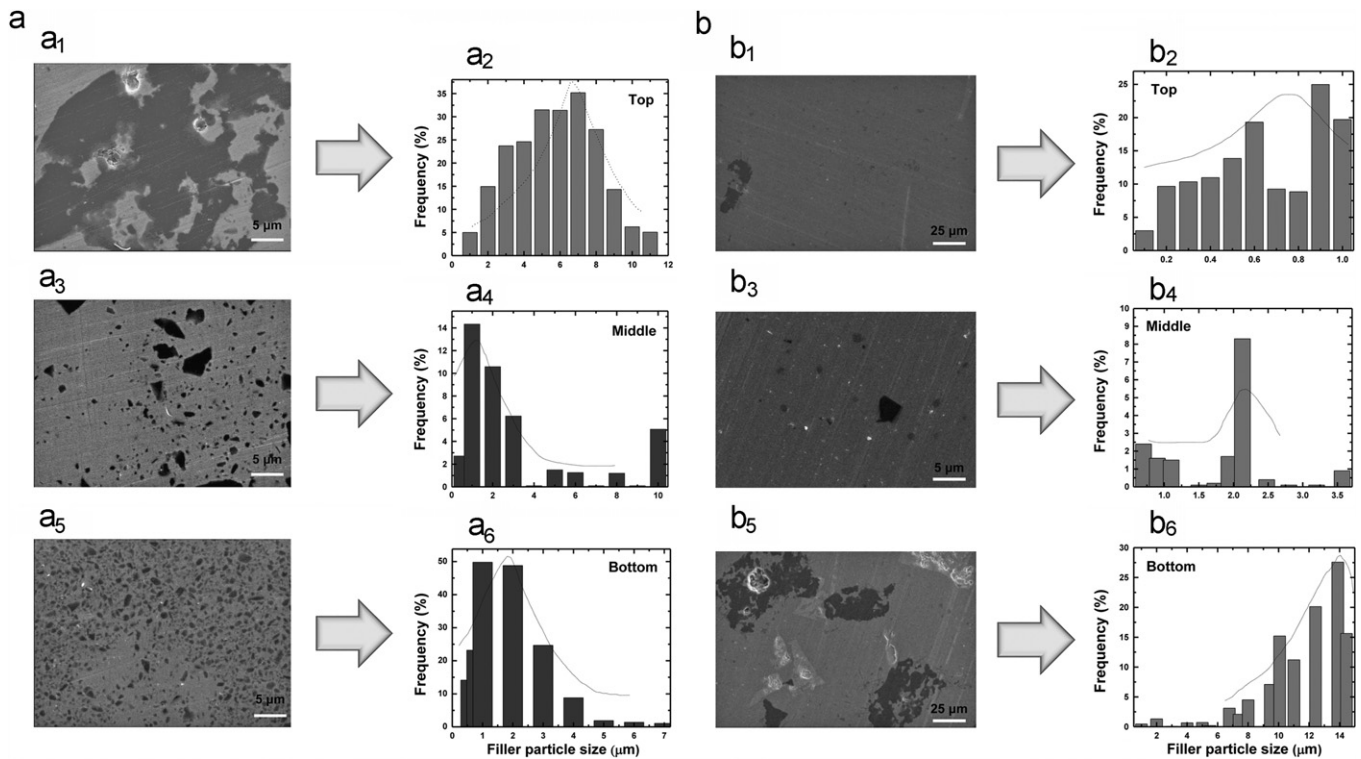


Fig. 6. (a) SEM micrographs of composites (a<sub>1</sub>, a<sub>3</sub> and a<sub>5</sub>) and filler distribution of composites (a<sub>2</sub>, a<sub>4</sub> and a<sub>6</sub>) sintered at 520 °C for a duration of 30 min. Upper portion of the composite ((a<sub>1</sub>)–(a<sub>2</sub>), major filler), middle portion of the composite ((a<sub>3</sub>)–(a<sub>4</sub>), uniform filler), and lower portion of the composite ((a<sub>5</sub>)–(a<sub>6</sub>), minor filler). (b). SEM micrographs of composites (b<sub>1</sub>, b<sub>3</sub> and b<sub>5</sub>) and filler distribution of composites (b<sub>2</sub>, b<sub>4</sub> and b<sub>6</sub>) sintered at 580 °C for a duration of 30 min. Upper portion of the composite ((b<sub>1</sub>)–(b<sub>2</sub>), major filler), middle portion of the composite ((b<sub>3</sub>)–(b<sub>4</sub>), uniform filler), and lower portion of the composite ((b<sub>5</sub>)–(b<sub>6</sub>), minor filler).

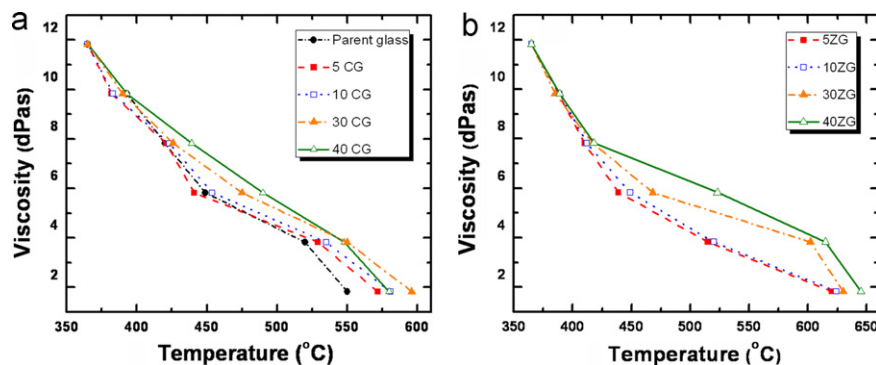


Fig. 7. (a). Viscosity–temperature curves obtained from HSM characteristics points for parent glass (without filler) and composites with various vol% of fillers (5, 10, 30, and 40) (CG: cordierite-glass) (b) Viscosity–temperature graphs from HSM characteristic points for composites at various vol% of fillers (5, 10, 30, and 40) (ZG: zinc oxide-glass).

results of the experiment with the glass composite with bimodal filler distribution. Fig. 9 shows the viscosity of the reactive (zinc oxide-glass composite) and non-reactive (cordierite-glass composite) system for unimodal and bimodal filler distributions of the composites. In the reactive system, the viscosity was observed to be significantly lower in the bimodal distribution than in the unimodal distribution. However, the viscosity was reduced with little variation in the non-reactive system of the glass composite. In the glass composite, the viscosity of the composite was lower with the bimodal fillers. These phenomena were confirmed by our results at the higher volume fraction. When the

composite had a crystalline nature, the viscosity appeared to increase and the fluidity was reduced. The results on the green and sintered composites at various volume fractions indicate that distinct peaks of the third phase developed during the interaction shown in Fig. 4. Higher concentrations of fillers can create pores that bridge between the particles, according to the theory proposed by Bordial et al. [8]; pores with the higher volume fraction were observed, as shown in Fig. 3(c).

According to the free volume theory, a glass system creates free volume at a higher temperature than  $T_g$  in the liquid stage [15,16]. The fluidity and densification increase

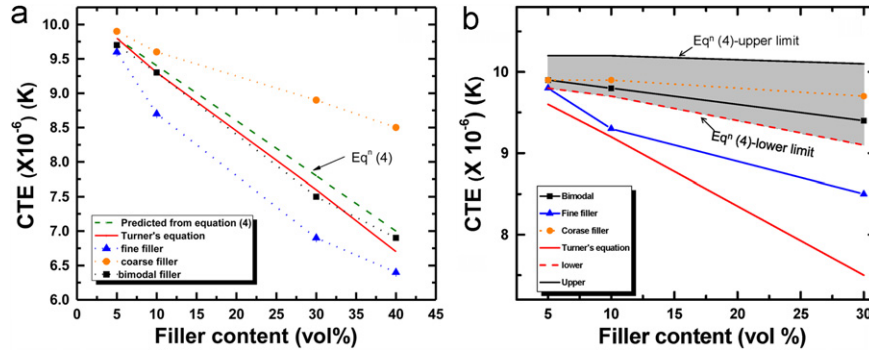


Fig. 8. CTE measurements as a function of filler type (coarse, fine, bimodal size fillers) with volume fraction in the composite: (a) Cordierite-glass composite (b) Zinc oxide glass composite Considering Eq. (3),  $\left\{ V_i = 3V_f \left( \frac{\Delta r_i}{r_f} \right) \right\}$ ,  $\Delta r_i = 1 \mu\text{m}$ ,  $r$  represents the radius,  $i$  and  $f$  represent the interface and filler, and  $\alpha$  represents the CTE.  $\alpha_i$  (lower limit)  $= 5 \times 10^{-6}$  and  $\alpha_i$  (upper limit)  $= 8 \times 10^{-6}$ .

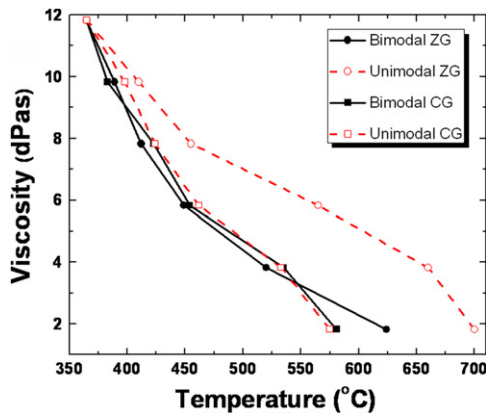


Fig. 9. Viscosity–temperature for the unimodal and bimodal distribution in the composites.

with the glass filler interacting system [17,18], which concur with the results for the zinc oxide composite shown in Fig. 5. Depending on the reactivity between glass and ceramic, which is classified as partial reactive, non-reactive, and complete reactive systems, the particle rearrangement within the composite at the liquid phase has been established in relation to the density of the filler. The reactive (zinc oxide-glass) and non-reactive (cordierite-glass) systems were observed to play an active role in the transport behavior of the thermal expansion of the composites. If the filler within the glass matrix is interactive, this principle does not follow for composites; this was observed in the zinc oxide filler. Zinc oxide shows a high degree of CTE when compared with cordierite.

The CTE for the composite can be calculated as follows

$$\alpha_c = \alpha_f V_f + \alpha_m V_m + \alpha_i V_i \quad (2)$$

The first two terms on the right hand side of the Eq. 2, relate to the filler and matrix of the composite. The third term relates to the third phase that was formed in the matrix.  $V_i$  is the volume fraction of the third phase (interphase) and can be represented as [18]

$$V_i = 3V_f \left( \frac{\Delta r_i}{r_f} \right) \quad (3)$$

By incorporating the value of Eq. (3) in Eq. (2), the CTE of the composite can be modified by the equation below

$$\alpha_c = \alpha_f V_f + \alpha_m V_m + 3V_f \left( \frac{\Delta r_i}{r_f} \right) \alpha_i \quad (4)$$

where the subscripts  $f$ ,  $m$  and  $i$  represent the filler, matrix and interphase.  $r$  represents the radius of filler,  $\Delta r_i$  represents the thickness of the interphase (change in radius from filler towards the glass matrix),  $V$  represents the volume fraction, and  $\alpha_i$  represents the CTE of the interface.

The Eq. (4) shows that the CTE of the composite ( $\alpha_c$ ) depends on three components the filler, the matrix, and the third phase-to-develop due to an interaction between the filler and glass matrix. Fig. 8(a) and (b) explain the comparison between the theoretical and experimental values. For the reactive (zinc oxide-glass) system, considering the value of  $\Delta r_i = 1 \mu\text{m}$ , with a lower ( $5 \times 10^{-6}/\text{K}$ ) limit and upper ( $8 \times 10^{-6}/\text{K}$ ) limit of  $\alpha_i$ , the net CTE of the composite was calculated (Fig. 8b). Assuming the values of the lower and upper limits for the interface, the CTE of the composite was calculated. CTE shows sound agreement between the theoretical value that was obtained from Eq. (4) and the theoretical value that was obtained from the experimental data, with variation from the lower to upper limits of the interfaces. The results indicate that the zinc oxide system affects the prediction of the CTE by the formation of a new phase around the zinc oxide filler.

The filler distribution in a glass matrix was explored on the basis of the study results deduced from Fig. 6. The filler arrangement for various sizes of the filler within the glass matrix during sintering is shown. Fig. 10 displays the distribution of fillers in a liquid glass matrix that correlates with physical and thermal factors, such as density and temperature. The density of fillers within the glass matrix plays a crucial role in the migration of fillers from the top to the bottom portion of the composite. The movement and distribution of fillers, in the liquid phase of the glass matrix of the composite, was examined in a sintering furnace at two different temperatures for a 30-min holding

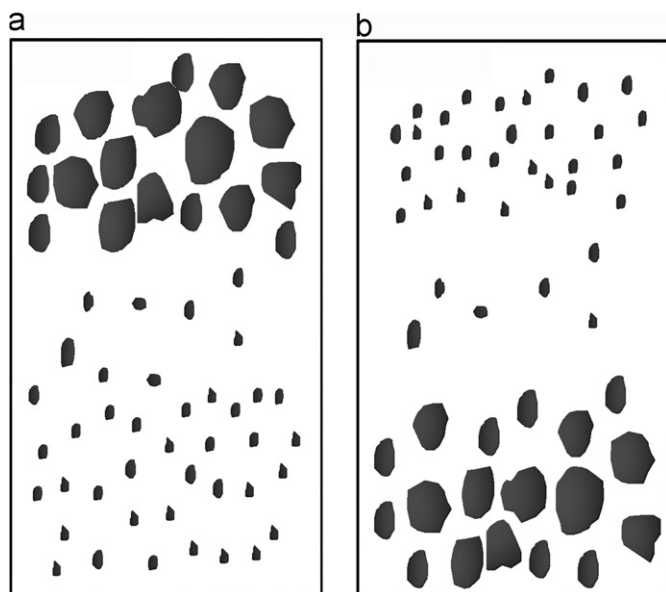


Fig. 10. Filler distribution at (a) 520 °C and (b) 580 °C in the liquid phase of the glass matrix based on Fig. 6.

period. A distribution that began as coarse near the top and changed to fine filler particles at the bottom was observed throughout the glass matrix in the composite at 520 °C (Fig. 10a).

The drift force acts on the filler particles (lower density) by moving them towards the upper portion of the composite while the glass matrix (higher density) moves downwards at the sintering temperature due to the gravitational force. At a higher temperature (580 °C), the filler distributions are opposite of the filler distributions at lower temperatures, and major coarse fillers are apparent in the bottom portion of the composite (Fig. 10b). The correlation between the viscosity and effect of the filler in the liquid phase of the composite has been established [19]. This drift phenomenon was observed in a non-reactive system such as cordierite-glass composite as opposed to the zinc oxide-glass reactive system. The non-reactive system exists without any binding forces between the filler and the glass; conversely, strong binding forces develop in the liquid phase of the reactive system.

Viscosity can be increased by using fillers with a narrow range of size distribution. The effect of density on the glass viscosity impacts the arrangement of filler in the glass matrix. The mechanism of sintering; however occurs by a combination of glass redistribution, grain rearrangement and viscous flow in the liquid phase of the glass matrix. Viscosity is a function of distribution of filler size in the composite. Viscosity depends on particle size, from fine to coarse, in the glass composite. The viscosity increases from fine filler distribution to coarse filler distribution in the glass matrix of the composites.

A bimodal filler distribution illustrates that the minimum viscosity results from the combination of fine and coarse particles as shown in Fig. 9. At a higher volume fraction, only bimodal filler in the composite displays the

best results. A high number of smaller particles results in more particle-particle interactions and an increased resistance to flow. This correlation indicates an increase in viscosity with an increase in volume fraction. As the maximum volume fraction is reached, the viscosity rises sharply because the free movement of the filler particles is significantly hindered due to frequent collisions between particles and a packed system. The incorporation of the bimodal cordierite filler system allows for a reduction in the viscosity and the CTE of the composite, thus improving the efficiency of the sealing material for special applications.

## 5. Conclusion

The viscosity is lower in cordierite-glass composite with bimodal filler distribution. In the case of zinc oxide-glass composite, the viscosity was also reduced at high temperatures due to the filler movement from the upper portion to the lower portion of the composite. Cordierite-glass composite is the non-reactive system, both viscosity and CTE reduced remarkably with bimodal filler distribution. Whereas the zinc oxide-glass composite is a fully reactive system, shows reduced viscosity but CTE increases. The density was found to play a crucial role in distribution and arrangement of the filler throughout the glass matrix at liquid phase in sintering temperature. The filler arrangement influences the viscous property of the composite from fine to coarse sizes in the matrix. The viscosity and CTE are dependent on the particle size and volume fraction of the filler. The bimodal distribution of the filler exhibits a reduced viscosity and lower CTE, which meets the desired characteristics and, therefore, is a good candidate for the packaging industry.

## Acknowledgment

This research effort was supported by the Pioneer Research Center of the National Research Foundation of Korea, funded by the Ministry of Education, Science and Technology (2011-0001685).

## References

- [1] A.R. Dinesen, D. Beeaff, P.H. Larsen, K.A. Nielsen, M. Solvang, S.B.L. Nielsen, Glass composite seals for SOFC application, *Journal of the European Ceramic Society* 27 (2007) 1817–1822.
- [2] B.E. O'Donnelly, Sealing Glass Composite, USA patent 5,284,706 (1994).
- [3] R. Arpon, J.M. Molina, R.A. Saravanan, C. Gracia-Cordovilla, E. Louis, J. Narciso, Thermal expansion behavior of aluminium/SiC composites with bimodal particle distributions, *Acta Materialia* 51 (2003) 3145–3156.
- [4] H.J.H. Brouwers, Particle-size distribution and packing fraction of geometric random packings, *Physical Review E* 74 (3) (2006) 031309-1-0313014.
- [5] H. Shin, S.G. Kim, J.S. Park, J.S. An, K.S. Hong, H. Kim, Co-Additions of TiO<sub>2</sub> and SiO<sub>2</sub> crystalline fillers to tailor the properties of BaO–ZnO–B<sub>2</sub>O<sub>3</sub>–SiO<sub>2</sub> glass for application to barrier

- ribs of plasma display panels, *Journal of the American Ceramic Society* 89 (10) (2006) 3258–3261.
- [6] S. Samal, S. Kim, H. Kim, Effects of filler size and distribution on viscous behavior of glass composites, *Journal of the American Ceramic Society* 95 (5) (2012) 1595–1603.
- [7] S.J. Milne, M. Patel, E. Dickinson, Experimental studies of particle packing and sintering behavior of monosize and bimodal spherical silica powders, *Journal of the European Ceramic Society* 11 (1993) 1–7.
- [8] R.K. Bordia, R. Raj, “Analysis of sintering of a composite with a glass or ceramic matrix”, *Journal of the American Ceramic Society* 69 (3) (1986) C-55–C-57.
- [9] W. Yang, S. Yu, R. Sun, R. Du, “Nano- and microsize effect of CCTO fillers on the dielectric behavior of CCTO/PVDF composites”, *Acta Materialia* 59 (2011) 5593–5602.
- [10] J.M. Molina, R.A. Saravanan, R. Apron, C. Gracia-Cordovilla, E. Louis, J. Narciso, Pressure infiltration of liquid aluminium into packed SiC particulate with a bimodal size distribution, *Acta Materialia* 50 (2002) 247–257.
- [11] J.M. Molina, J. Narciso, L. Weber, A. Mortensen, E. Louis, Thermal conductivity of Al-SiC composites with monomodal and bimodal particle size distribution, *Materials Science and Engineering: A* 480 (2008) 483–488.
- [12] R.K. Goyal, A.N. Tiwari, U.P. Mulik, Y.S. Negi, Thermal expansion behavior of high performance PEEK matrix composites, *Journal of Physics D: Applied Physics* 41 (2008) 1–7.
- [13] M. Foroutan, Density dependence of the viscosity and excess volume of aqueous solutions of polyvinylpyrrolidone, *Acta Chimica Slovenica* 53 (2006) 219–222.
- [14] A.J. Poslinski, M.E. Ryan, R.K. Gupta, S.G. Seshadri, F.J. Frechette, Rheological behavior of filled polymeric systems II. The effect of a bimodal size distribution of particulates, *Journal of Rheology* 32 (8) (1988) 751–771.
- [15] C.L. Chen, W. Cheng, J. Wei, A. Roosen, Wetting, densification and phase transformation of  $\text{La}_2\text{O}_3/\text{Al}_2\text{O}_3/\text{B}_2\text{O}_3$ -based glass-ceramics, *Journal of the European Ceramic Society* 26 (2006) 59–65.
- [16] M.H. Cohen, G.S. Grest, A new free-volume theory of the glass transition, *Annals of the New York Academy of Sciences* 371 (1) (2006) 109–209.
- [17] A.K. Mukhopadhyay, S. Neekhara, D.G. Zollinger, Preliminary characterization of aggregate coefficient of thermal expansion and gradation for paving concrete, Report no. FHWA/TX-05/0-1700-5, 2007, pp. 1–124.
- [18] N. Lombardo, Effect of an inhomogeneous interphase on the thermal expansion coefficient of a particulate composite, *Composites Science and Technology* 65 (2005) 2118–2128.
- [19] Y. Huang, D. Bigio, M.G. Pecht, Investigation of the size and spatial distribution of fillers in mold compounds after device packaging, *IEEE Transactions on Components and Packaging Technologies* 29 (2) (2006) 364–370.